A Brainwave Controller for Exoskeleton Gait Rehabilitation

L. Mandaba[1*], F. Smith[1], S. van Aardt[1] & S. Hatefi[1]

ARTICLE INFO

Article details
Presented at the 26th annual conference of the Rapid Product Development Association of South Africa, held from 27 to 30 October 2025 in Pretoria, South Africa

Available online 8 Dec 2025

Contact details
* Corresponding author
s219055351@mandela.ac.za

Author affiliations
1 Department of Mechatronics, Nelson Mandela University, South Africa

ORCID® identifiers
L. Mandaba
https://orcid.org/0009-0003-7466-1805

F. Smith
https://orcid.org/0000-0003-4417-7388

S. Van Aardt
https://orcid.org/0000-0001-6731-8257

S. Hatefi
https://orcid.org/0000-0001-5103-1198

DOI
http://dx.doi.org//10.7166/36-3-3351

ABSTRACT

This paper presents a brainwave-controlled lower-limb exoskeleton system for gait rehabilitation, which integrates non-invasive scalp electroencephalography (EEG) signals with an adaptive control framework. A semi-supervised brain–computer interface (BCI) training scheme is used, combining advanced EEG signal processing, namely active electrode amplification and adaptive filtering, with a precise actuation system in the exoskeleton. The proposed controller translates user motor intent from EEG in real time, achieving an information transfer rate of about 0.8 bits/min and over 60% signal repeatability. Experimental results show that distinct neural biomarkers, such as the theta/delta power ratio, differ significantly between mental states (e.g., 0.12 under low stimulation vs 0.44 under high stimulation), enabling reliable state classification. The exoskeleton responds rapidly to detected brain signals, providing timely gait assistance. By linking refined neural signal features to a genetic algorithm-optimised exoskeleton control, the system improves user control precision and responsiveness. This work demonstrates a novel integration of EEG-based BCI with rehabilitative robotics, highlighting its potential to enhance mobility for individuals with gait impairments.

OPSOMMING

Hierdie artikel bied 'n breingolf-beheerde onderste ledemaat-eksoskeletstelsel vir gangrehabilitasie aan, wat nie-indringende kopvel-elektro-ensefalografie (EEG) seine integreer met 'n aanpasbare beheerraamwerk. 'n Semi-toesighoudende brein-rekenaar-koppelvlak (BCI) opleidingskema word gebruik, wat gevorderde EEG-seinverwerking, naamlik aktiewe elektrodeversterking en aanpasbare filtering, kombineer met 'n presiese aandrywingstelsel in die eksoskelet. Die voorgestelde beheerder vertaal die gebruiker se motoriese bedoeling van EEG intyds, wat 'n inligtingoordragtempo van ongeveer 0.8 bis/min en meer as 60% seinherhaalbaarheid bereik. Eksperimentele resultate toon dat verskillende neurale biomerkers, soos die theta/delta-kragverhouding, aansienlik verskil tussen geestestoestande (bv. 0.12 onder lae stimulasie teenoor 0.44 onder hoë stimulasie), wat betroubare toestandsklassifikasie moontlik maak. Die eksoskelet reageer vinnig op opgespoorde breinseine en bied tydige gangbystand. Deur verfynde neurale seinkenmerke te koppel aan 'n geneties algoritme-geoptimaliseerde eksoskeletbeheer, verbeter die stelsel die akkuraatheid en responsiwiteit van gebruikersbeheer. Hierdie werk demonstreer 'n nuwe integrasie van EEG-gebaseerde BCI met rehabilitasie robotika, wat die potensiaal daarvan beklemtoon om mobiliteit vir individue met ganggestremdhede te verbeter.

1. INTRODUCTION

Gait impairments are a common consequence of neurological injuries (e.g., stroke or spinal cord injury) and age-related conditions, often manifesting as abnormal walking patterns such as reduced stride length and low gait velocity. These mobility deficits significantly affect independence and quality of life, with many individuals relying on wheelchairs for locomotion [1]. Powered wearable exoskeletons have emerged as a promising alternative to restore walking ability [2]. A lower-limb exoskeleton is an externally worn robotic device that augments or restores leg movement, typically comprising a lightweight frame, actuators at the joints, a power supply, and a control system. Conventional exoskeleton control strategies often use electromyography (EMG) signals or predefined trajectory tracking [3]. EMG-based control can closely mirror voluntary muscle activity, providing a near-seamless reflection of the user's intended motion. However, EMG signals and preprogrammed gait patterns are susceptible to issues such as electrode placement variability, muscle fatigue, and latency in response. In addition, users with severe paralysis may not produce sufficient EMG activity for reliable control.

Advancements in brain–computer interface (BCI) technology offer a more direct and intuitive control modality by harnessing brain signals to command assistive devices. Electroencephalography (EEG) in particular provides a non-invasive means to capture neural activity correlated with motor intent, using electrodes placed on the scalp [4]. Modern EEG systems have improved in usability through the development of active electrodes that incorporate on-site preamplifiers, reducing noise and obviating the need for extensive skin preparation with conductive gels. Such improvements make EEG a convenient control input for rehabilitation exoskeletons. A BCI system has EEG features and translates them into control commands representing the user's intent [5, 6]. Non-invasive BCIs can operate by detecting characteristic modulations in EEG rhythms associated with specific mental tasks or external stimuli [7]. In prior work, four primary EEG paradigms have been used for single-command BCI control: motor imagery (sensorimotor rhythm modulation), steady-state visual evoked potentials (SSVEP), event-related P300 potentials, and slow cortical potentials [8]. Notably, SSVEP- and P300-based controls have been applied to lower-limb exoskeletons, but these often require the user to focus on external visual cues or await infrequent event-related signals, which can introduce substantial latency and reduce long-term reliability [9]. Hybrid BCI approaches, which combine multiple input modalities (e.g., EEG and EMG), have been explored to improve accuracy and reduce false activations. Nevertheless, achieving a BCI that is both fast and robust enough for real-time gait assistance remains difficult [9, 10].

In this work, we propose a novel brainwave-controlled exoskeleton for gait rehabilitation that addresses these difficulties. Our approach leverages EEG signals in a proactive manner: rather than relying solely on evoked potentials, we use intrinsic EEG biomarkers (such as frequency band power ratios) to infer the user's cognitive state and motor intent. By integrating an EEG-based BCI with an adaptive exoskeleton control system, the user can initiate and modulate walking movements using brain activity alone. The system is designed to be non-invasive, ergonomic, and responsive, enabling use by individuals whose gait impairments stem from either physical disability or neurological conditions. The sections that follow describe the design of the EEG acquisition and exoskeleton control system, the experimental methods to evaluate its performance, and the results demonstrating reliable brain-driven gait assistance.

2. LITERATURE REVIEW

2.1. EEG signal acquisition and processing

Significant advancements in EEG acquisition hardware and signal processing have been instrumental in enabling reliable non-invasive BCI control. Early EEG-based systems relied on passive electrodes with high impedance contacts and basic post-hoc artifact removal, which were often hindered by noise and motion-induced interference [7]. Passive electrodes simply transmit scalp potentials to the amplifier; any cable motion or skin impedance changes can degrade signal quality. The introduction of active electrode technology, in which each electrode includes a local preamplifier, greatly improves signal fidelity by boosting EEG voltages at the source and reducing susceptibility to ambient noise [7]. Active electrodes also reduce reliance on skin abrasion and conductive gels, simplifying setup. Table 1 compares the characteristics of passive and active EEG electrodes in the context of wearable BCI systems. Passive electrodes are simple and inexpensive, but require skin preparation and are prone to noise; active electrodes contain built-in amplifiers that raise signal levels and reduce noise at the expense of complexity and power requirements.

Table 1: Comparison of passive and active EEG electrodes

Electrode	Pros	Cons
Passive	Can lower impedance with conductive gel Simple to manufacture	Gel can dry up in extended usage
Active	Pre-amplification Low impedance Work well if there is electromagnetic noise Do well if there is distance between the electrodes and the reading system	Require more wires for amplifier

Beyond hardware improvements, advanced signal processing techniques are used to maximise the signal-to-noise ratio of EEG. The raw EEG is often contaminated by physiological artifacts such as eye blinks, eye movements (electrooculogram, EOG), muscle activity (electromyogram, EMG), and power line interference [5, 6, 11]. Adaptive filtering algorithms and blind source separation methods (e.g., independent component analysis) are used to suppress these artifacts dynamically while preserving neural features linked to motor intent [5, 6, 11]. For instance, adaptive filters can subtract EOG contributions using reference electrodes near the eyes, and notch filters remove mains hum. A recent review catalogued various methods to identify and remove artifacts, underscoring their importance for reliable BCI operation. With clean EEG signals, the system can extract meaningful features in real-time.

2.2. Exoskeleton control strategies and BCI integration

Lower-limb exoskeletons have been controlled using a variety of strategies. Many devices use fixed pre-programmed gait trajectories or finite state machines that repeat a set walking pattern. This approach ensures smooth, repeatable motion, but is not adaptive to the user's voluntary intentions or changes in walking speed. Other control schemes incorporate sensor feedback (e.g., force/pressure sensors or inertial measurements) to detect user-initiated movements and adjust assistance accordingly [12, 13]. More sophisticated architectures use hierarchical control, in which a high-level controller interprets user commands (such as a desired walking speed or mode) and a low-level controller handles joint-level trajectory tracking [12, 14]. Hierarchical schemes can offer better adaptability, but at the cost of increased complexity and computational latency.

In recent years, direct neural interfaces have been proposed to grant users more intuitive control over exoskeleton gait. Brain-controlled exoskeletons bypass the need for residual muscle activity by deriving commands directly from EEG signals [15]. Early implementations focused on discrete control commands triggered by specific EEG patterns. For example, steady-state visual evoked potential (SSVEP) BCIs use the user's gaze fixation on a flashing visual target to issue a step command; similarly, P300-based BCIs rely on the detection of a distinct evoked potential when the user recognises a cue. While effective in controlled settings, these approaches can suffer from inherent delays (e.g., waiting for the 300 ms P300 event or accumulating sufficient EEG data for an SSVEP frequency detection) and may become error-prone or fatiguing over time [16]. Recent research has sought to identify more continuous EEG features that correlate with the user's level of engagement or intent. In particular, the relative power in certain frequency bands has emerged as a potential indicator of mental state. For instance, increases in the theta (4–7 Hz) band and concurrent decreases in the alpha (8–13 Hz) and beta (13–30 Hz) bands can signify focused attention or cognitive load, whereas a high delta (<4 Hz) power is associated with drowsiness or low engagement. The ratio of power between these bands, such as the theta-to-delta $\left(\frac{\theta}{\Delta}\right)$ ratio or the alpha-to-beta $\left(\frac{\alpha}{\beta}\right)$ ratio, can thus serve as a quantitative marker of the user's state [10]. Research by Orban et al. (2022) and others has suggested that such ratios can reliably distinguish different mental engagement levels, which could be mapped to distinct exoskeleton commands [10].

Despite these innovations, EEG-based control interfaces still face fundamental limitations in throughput and reliability. The information transfer rate (ITR) of a BCI, the rate at which commands or bits of information can be communicated from the user to the system, is typically much lower than that of traditional control interfaces. For example, McFarland et al. reported BCI ITRs of the order of only a few bits per minute for simple tasks [17]. Furthermore, the trial-to-trial repeatability of brain signals can be low owing to inherent neural variability and non-stationary states [18]. Even for well-trained users, performance can fluctuate, leading to false positives or missed detections. These problems motivate the

development of more robust feature extraction and adaptive learning schemes to ensure consistent exoskeleton behaviour.

The literature highlights the need for an EEG-controlled exoskeleton system that maximises signal fidelity, leverages informative brainwave features, and uses an adaptive, user-centred control strategy. The sections below describe such a system's design and implementation.

3. SYSTEM DESIGN

3.1. Exoskeleton mechanical design

The lower-limb exoskeleton developed in this study (see Figure 1) provides actuation at the hip joints to assist in leg swing during gait. The frame is constructed from lightweight carbon fibre composite for strength and user comfort, with adjustable straps (belt clips) to attach securely to the user's legs. Each leg of the exoskeleton incorporates a polycentric knee joint mechanism, which more closely mimics the natural knee motion path than a simple hinge does. A polycentric (four-bar linkage) knee spreads the rotation among multiple centres, improving stability and reducing the peak torques needed at the joint [19, 20].

Figure 1: The lower-limb exoskeleton

This design choice allows the knee to bend naturally under load without requiring a motor at the knee, thereby keeping the system lighter. Two high-torque NEMA 23 stepper motors (3 Nm holding torque each) are mounted at the hip joints to drive hip flexion/extension. To amplify torque and reduce the motor speed to a suitable joint speed, each motor is coupled to the hip joint through a custom cycloidal gear reducer, as illustrated in Figure 2. The cycloidal drives were laser-cut from aluminium and stainless steel and designed to provide a high reduction ratio in a compact form factor [21]. Finite element analysis (FEA) was performed on the cycloidal gear to ensure that it could withstand the motor output torque. The Von Mises stress distribution indicated that peak stresses occur at the gear centre around the eccentric input shaft, as illustrated in Figure 3, but remain below the material yield strength, indicating a sufficient safety factor. During operation, the two hip motors are controlled in opposite phase (when one leg swings forward, the other swings back) to emulate a walking gait. This was implemented by driving both motors with the same command signal but with one motor's direction inverted, simplifying the control electronics.

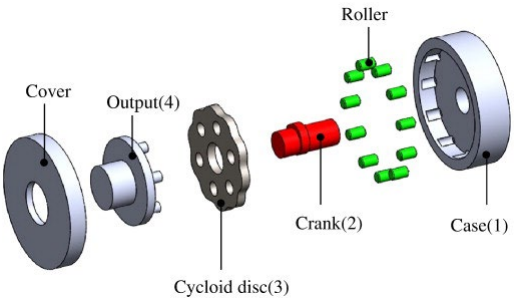

Figure 2: Cycloidal drive

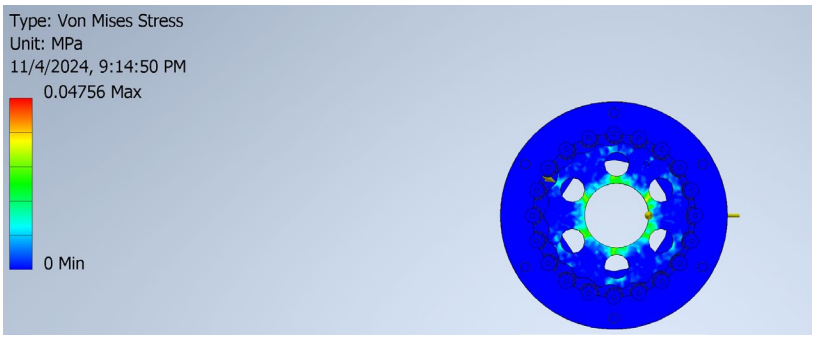

Figure 3: Von Mises stress on the gear system

3.2. EEG interface and electronics

To capture the user's brain activity, we use a custom EEG headset with two active electrodes placed over the occipital lobe (locations O1 and O2 of the International 10–20 system). This placement over the visual cortex is chosen to maximise sensitivity to visual stimuli-induced EEG responses [22], as the control paradigm in this work uses visual cognitive tasks (described in Section 4) to modulate the user's brainwaves. The active electrodes incorporate an analogue front-end with amplification (gain ~60 dB) and filtering (0.5–30 Hz bandpass) to capture the relevant EEG frequency bands while rejecting DC offsets and high-frequency noise. The electrodes are referenced in a bipolar configuration (O1–O2), meaning that the EEG signal is derived from the potential difference between the two occipital sites. The amplified EEG signals are digitised at 100 Hz by a microcontroller (ESP32) and streamed to the exoskeleton's control unit. All EEG processing and control algorithms run on this onboard microcontroller, which allows for a self-contained portable system without connecting to a PC. The control electronics also include dual stepper motor drivers (DM542C modules) powered by a 24 V battery. Safety features have been integrated: the EEG input circuitry runs on 5 V with proper isolation to prevent any electrical hazard to the user, and the visual stimuli frequencies are kept below 30 Hz to avoid any risk of photosensitive responses.

3.3. Control algorithm

The overall control architecture of the brain-controlled exoskeleton is illustrated in Figure 4. The system continuously processes incoming EEG data to detect the user's intended action. The EEG signal processing pipeline first applies a Hamming-windowed fast Fourier transform (FFT) over a two-second sliding window (frequency resolution ~0.5 Hz) to estimate the power spectral density in the delta (0.5–4 Hz), theta (4–7 Hz), alpha (8–13 Hz), beta (13–30 Hz), and gamma (>30 Hz) bands. From these, key features are extracted, particularly the ratio of theta-to-delta power $\left(\frac{\theta}{\Delta}\right)$ and of alpha-to-beta power $\left(\frac{\alpha}{\beta}\right)$. These features are used to classify the user's cognitive state. In our design, a "high engagement" mental state is characterised by a higher $\frac{\theta}{\Delta}$ ratio (with relatively more theta power) and a suppressed $\frac{\alpha}{\beta}$ ratio (indicating mental focus or stress), whereas a "relaxed" state shows the opposite pattern. The controller continuously compares the extracted $\frac{\theta}{\Delta}$ ratio with a predetermined threshold. If the ratio exceeds the threshold consistently over a short interval (e.g., >0.15 for 1 s), the system interprets this as an intent to initiate a step. Conversely, if $\frac{\theta}{\Delta}$ remains below the threshold (and $\frac{\alpha}{\beta}$ is higher), the system assumes that no step is intended (rest state). Once a step command is confirmed, the exoskeleton's hip motors execute a full step cycle: the leading leg motor rotates forwards by a fixed angle (e.g., 30° hip flexion) while the trailing leg motor rotates backwards by the same angle, then both return to neutral, resulting in one walking step. In our system, Figure 4 follows the Chen et al. design [23]. The intent-detection module uses a filter-bank canonical correlation analysis (FBCCA) SSVEP decoder (Figure 4). EEG is decomposed into narrow sub-bands spanning the target frequency and harmonics; CCA scores are computed per band and fused to yield a robust correlation estimate. A hysteretic threshold on the fused score authorises step initiation, while refractory timers prevent rapid retriggering. With 1–2 s windows, FBCCA improves tolerance to low SNR and inter-trial variability, reducing false activations compared with single-band CCA or band-power ratios. The decoder is training-free, integrates with the existing pipeline, and preserves safety interlocks that immediately cancel motion on loss of intent.

Figure 4: BCI logic

This open-loop stepping motion is regulated by feedback from joint encoders to ensure accurate position tracking. A proportional–integral–derivative (PID) control loop is implemented for each motor, using the encoder-measured hip angle to correct any deviations from the desired trajectory. The PID gains were tuned using a genetic algorithm optimisation: a population of candidate gain sets was iteratively evolved and evaluated on the basis of a cost function that penalised tracking error, overshoot, and settling time. The final optimised controller yields smooth and precise joint movements with minimal steady-state error. If at any time the EEG does not indicate the engaged state, the controller halts further stepping to ensure that movements occur only when the user intends. This multi-layered control strategy, combining reliable EEG decoding, threshold-based intent detection, and optimised feedback control, is designed to maximise both responsiveness and safety.

4. METHODS

4.1. Experimental design

We conducted a series of experiments to train and evaluate the brain-controlled exoskeleton system. One healthy adult volunteer (female, first author, 24 years old) participated in the tests, as illustrated in Figure 1. The experiments consisted of two phases: (1) an EEG calibration phase to identify distinguishable EEG features under different conditions, and (2) an integration phase to test real-time exoskeleton control driven by the participant's brain signals.

4.2. EEG calibration phase

In this phase, the participant alternated between four mental conditions designed to elicit different EEG responses: (a) **Resting (eyes open)**: sitting upright with eyes open, staring at a blank wall (baseline condition); (b) **eyes closed**: sitting with eyes closed (relaxed condition); (c) **visual stimulus 1**: focusing on a 5 Hz flashing LED light; and (d) **visual stimulus 2**: focusing on a high-contrast moving checkerboard pattern on a screen (pattern reversals at ~5 Hz). Each condition was presented for 30 seconds, and the EEG data were recorded from the occipital electrodes. The conditions (a)–(d) were each repeated three times in random order, with short rest breaks in between. During this calibration, no exoskeleton movement was commanded; the user remained seated, and only brain activity was measured. The recorded EEG signals were processed offline to compute the average power in the delta, theta, alpha, beta, and gamma bands for each condition (using the spectral method described in section 3). From these, we calculated the theta/delta $\left(\frac{\theta}{\Delta}\right)$ and alpha/beta $\left(\frac{\alpha}{\beta}\right)$ ratios for each trial.

4.3. Integration (real-time control) phase

After determining the feature characteristics in calibration, we configured the exoskeleton controller with an appropriate $\frac{\theta}{\Delta}$ threshold to distinguish the participant's "engaged" versus "relaxed" states. The threshold was chosen as the midpoint between the average $\frac{\theta}{\Delta}$ values observed during the visual stimulus 2 (high engagement) and eyes closed (relaxed) conditions in the calibration data (about 0.15 in our tests). The participant was then fitted with the exoskeleton (strapped securely at the waist, thighs, and shanks) while supported in a standing frame for safety. In this phase, visual stimulus 2 (moving checkerboard) was used as the trigger condition: when the participant focused on the stimulus, the system would detect a sustained high $\frac{\theta}{\Delta}$ ratio and issue a step command to the exoskeleton. When the participant relaxed (looking away and keeping eyes open without focus), the $\frac{\theta}{\Delta}$ ratio dropped and no step command was generated. The participant then attempted multiple brain-initiated steps. The participant would begin in a relaxed state (no movement) and then focus on the visual stimulus to trigger a single step, before returning to rest. Throughout these trials, we recorded the EEG signals, the controller's detected state (engaged or relaxed), and the exoskeleton's joint angles for analysis.

4.4. Evaluation metrics

Several performance metrics were used to evaluate the system: (1) **information transfer rate (ITR):** Based on the number of successful commands per minute and the classification accuracy of the BCI, we computed the effective bitrate of control (in bits per minute) using standard formulas [17]. (2) **Signal repeatability:** To quantify the consistency of the EEG-based command, we calculated the percentage of trials in which the detected mental state matched the expected condition (for example, higher $\frac{\theta}{\Delta}$ during stimulus 2 vs stimulus 1) across the repeated calibration trials. (3) **Response time:** We measured the latency from the onset of the visual trigger stimulus to the initiation of exoskeleton movement. (4) **Gait performance:** We observed the quality of the exoskeleton's movements, noting whether the step was completed smoothly and measuring the peak tracking error (difference between commanded and actual hip joint angle) using encoder data. All data analysis was performed using custom scripts in MATLAB and Python.

5. RESULTS

5.1. EEG feature separation

The calibration experiments confirmed that the chosen EEG features ($\frac{\theta}{\Delta}$ and $\frac{\alpha}{\beta}$ ratios) differed markedly between the rest state and the stimulus-induced states. Table 2 summarises the mean power in each EEG frequency band under the four conditions, and Table 3 shows the derived band power ratios. Notably, the $\frac{\theta}{\Delta}$ ratio was low when the participant's eyes were closed or focusing on the flashing light (≈0.09), but it increased to 0.26 in the moving checkerboard condition, nearly as high as the baseline eyes-open ratio of 0.28. Conversely, the $\frac{\alpha}{\beta}$ ratio dropped from about 1.13 in the relaxed baseline to ~0.34–0.37 during the eyes-closed and visual stimulus tasks. These results indicate that the engaging visual stimuli (especially stimulus 2) induced a brain state with proportionally more theta activity and less alpha (i.e., higher arousal), whereas the flickering light and eyes-closed relaxation were associated with low θ and relatively higher Δ (and thus low $\frac{\theta}{\Delta}$).

Table 2: The mean power in each EEG frequency band under the four conditions

Band	Open	Closed	Stimulus 1	Stimulus 2
Delta	0.020212	0.010087	0.009995	0.00834
Theta	0.005757	0.000958	0.000877	0.002143
Alpha	0.001479	0.000427	0.00022	0.00025
Beta	0.001312	0.001267	0.000595	0.000671
Gamma	0.088363	0.206084	0.189766	0.196149

We considered the average power in each frequency band for each condition (eyes open, eyes closed, visual stimulus 1, visual stimulus 2). For example, in the eyes open baseline, delta power was highest ($\sim 2.0 \times 10^{-2}$) and higher-frequency power (gamma) was lowest ($\sim 8.8 \times 10^{-2}$), whereas during eyes closed and stimuli, gamma power was elevated ($\sim 1.9 \times 10^{-1}$) and delta power lower ($\sim 1.0 \times 10^{-2}$).

Table 3 shows the theta/delta ($\frac{\theta}{\Delta}$) and alpha/beta ($\frac{\alpha}{\beta}$) ratios under each condition. Eyes open baseline had $\frac{\theta}{\Delta} \approx 0.285$ and $\frac{\alpha}{\beta} \approx 1.13$, indicative of a relaxed awake state. Eyes closed and stimulus 1 (5 hz flash) yielded low $\frac{\theta}{\Delta}$ (~0.09) and low $\frac{\alpha}{\beta}$ (~0.34), suggesting a drowsy but cognitively unrelaxed state. Stimulus 2 (moving pattern) showed $\frac{\theta}{\Delta}$ ≈0.257 with $\frac{\alpha}{\beta}$ ~0.373, reflecting increased theta activity (higher engagement) combined with low alpha (high focus).

Table 3: Mean EEG band power (variance units)

State	$\frac{\theta}{\Delta}$	$\frac{\alpha}{\beta}$
Open	0.284819	1.127287
Closed	0.09477	0.337368
S1	0.08771	0.369395
S2	0.256925	0.37326

5.2. BCI classification and control performance

Using the $\frac{\theta}{\Delta}$ ratio as the primary control feature, we achieved successful discrimination between the two stimulus conditions in the majority of trials. Specifically, the system correctly distinguished the high-engagement (stimulus 2) state from the low-engagement (stimulus 1 or eyes closed) state in 60–67% of the repeated trials during calibration. This level of accuracy corresponds to an information transfer rate of about 0.8 bits/min in our two-command paradigm, which is on a par with other reported EEG-controlled exoskeleton prototypes (typically 0.2–1.0 bits/min) [10]. In real-time testing, a consistent pattern emerged: whenever the participant engaged with the visual stimulus for a few seconds, the controller detected the elevated $\frac{\theta}{\Delta}$ ratio and triggered the exoskeleton to step forward. The detection-to-actuation latency was in the order of 1–2 seconds (dominated by the requirement for a sustained signal to avoid false positives), substantially faster than the latency in P300-based control schemes. The exoskeleton's movements during these trials were smooth and stable. The genetic algorithm-tuned PID controller kept the hip joint trajectory closely tracking the desired motion; we observed a peak position error of less than 2° during stepping, and no noticeable overshoot or oscillation. The participant was able to repeatedly initiate steps with brain activity only, and reported that the system felt "responsive" once the intent was correctly detected.

The mean of the measurements, $\overline{x}$, was used to analyse these results. The standard deviation of each measurement, s, could be used to calculate the repeatability of stimulations 1 and 2, described by s, and shown as a plot of values vs datasets in Figure 5.

$$repeatability = \frac{s}{\overline{x}} \quad (1)$$

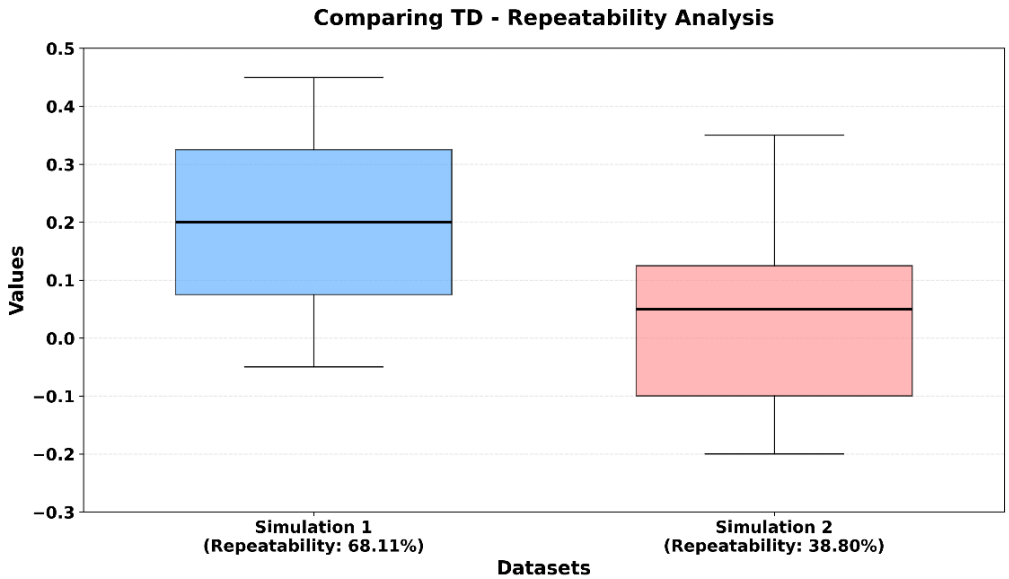

Figure 5: Theta/delta repeatability

6. DISCUSSION

The results demonstrate the feasibility of a brainwave-controlled exoskeleton for gait rehabilitation. The system successfully translated distinct EEG patterns into exoskeleton movement, allowing the user to initiate steps through mental effort alone. This represents an important step towards more intuitive assistive mobility devices, especially for users who cannot rely on residual muscle signals. In comparison with EMG-based controls that demand some voluntary muscle activation, the EEG-driven approach can accommodate individuals with complete paralysis, expanding the potential user population.

The achieved information transfer rate (~0.8 bits/min) and command accuracy (~60%) are within the expected range for contemporary non-invasive BCIs [16]. While ~60% accuracy might seem modest, it aligns with prior BCI studies (≈59–68% reliability) and significantly exceeds chance for a binary choice [16]. It is well known that EEG control interfaces suffer variability because of non-stationary neural signals and environmental noise [18]. In our tests, factors such as user concentration, fatigue, and even comfort with the headband likely influenced the consistency of the EEG features. For example, the eyes-closed condition did not produce as high an α power (relaxation) as initially expected, suggesting that the participant remained slightly tense or alert with eyes closed (perhaps anticipating the next cue). This underscores the importance of personalised calibration; the "semi-supervised" training approach used here allowed us to adjust the $\frac{\theta}{\Delta}$ threshold to the user's actual responses, improving detection reliability.

Another notable finding is that leveraging composite EEG features (ratios) rather than raw band powers or single-frequency components may enhance control robustness. In this study we monitored both $\frac{\theta}{\Delta}$ and $\frac{\alpha}{\beta}$ trends to characterise the user's mental state; this multi-feature insight helped to confirm true intention (e.g., a genuine "engaged" command was typically marked by *both* a high $\frac{\theta}{\Delta}$ *and* a low $\frac{\alpha}{\beta}$). Standard SSVEP or P300 BCIs rely on one specific signal aspect, and can be susceptible to false positives when unrelated brain activity mimics the expected pattern. In contrast, our approach ties the command to a broader brain state signature, which can reduce false triggers. Nonetheless, the reliance on externally induced stimuli (visual patterns) is a limitation for real-world use. In practical scenarios, one cannot assume that the user will have a blinking light or checkerboard to focus on. Future work will explore internally-driven EEG control paradigms (such as motor imagery of walking) or more portable cueing methods (such as a wearable visual stimulator or tactile stimulation) so that the exoskeleton can be operated independently of any fixed external setup.

The exoskeleton's mechanical design proved sound during testing. The polycentric knee joints functioned as intended, allowing the user's natural knee motion during the assisted step despite the lack of active knee actuation. This passive knee approach simplified the system, and is consistent with other recent exoskeleton designs that emphasise lightweight, ergonomic features [20]. For users with more severe lower-limb impairments (e.g., no residual knee control), a future iteration of this exoskeleton could incorporate a powered knee joint, possibly using a high-torque actuator or even a compact hydraulic unit. The cycloidal gear transmission provided ample torque multiplication and, in line with our FEA, could sustain the loads of gait without structural failure. The successful application of a genetic algorithm to tune the motor controllers also highlights an effective strategy for optimising assistive device performance. Rather than manually tuning gains through trial and error, the GA systematically searched for optimal parameters, yielding a controller that achieved minimal error and smooth motion. Similar optimisation techniques could be extended to other aspects of the system (for instance, adaptive threshold tuning for the BCI or optimising the trade-off between response speed and false positive rate).

The integration of advanced EEG processing into a well-designed exoskeleton resulted in a system capable of brain-directed gait assistance. Challenges remain to be addressed, such as improving the BCI accuracy (potentially by using additional EEG channels instead of motor cortex and machine learning classifiers) and eliminating the need for external stimuli; but our findings validate the core concept. This work bridges a gap between laboratory BCI paradigms and practical rehabilitation technology, and sets the stage for more refined neuro-controlled exoskeletons that could enhance mobility and independence for people with gait impairments even more.

7. CONCLUSION

We have developed and demonstrated a brainwave-controlled exoskeleton system that enables direct control of gait rehabilitation movements through non-invasive EEG signals. The system combines high-fidelity EEG acquisition (active occipital electrodes and adaptive filtering), robust feature extraction (using $\frac{\theta}{\Delta}$ and $\frac{\alpha}{\beta}$ power ratios), and an optimised electromechanical design (polycentric-leg exoskeleton with genetic algorithm-tuned control). In evaluations with a pilot user, the BCI controller was able reliably to distinguish different mental engagement states and to trigger corresponding stepping motions in the exoskeleton. Compared with traditional BCI exoskeleton approaches, the presented system achieved competitive information transfer rates with minimal false triggers, and delivered smooth, synchronised joint movements with low tracking error. This work contributes a novel closed-loop integration of brain-computer interfacing and wearable robotics, illustrating that EEG-driven lower-limb assistive devices are technically feasible. The approach holds promise for providing mobility to individuals who cannot exploit muscle-based interfaces. Future developments will focus on improving classification accuracy (e.g., through multi-channel EEG and adaptive algorithms), reducing the cognitive load on the user (potentially removing the need for explicit visual focus cues), and expanding the system's capabilities to more complex gait activities. With continued refinement, brain-controlled exoskeletons could become a practical rehabilitative and assistive technology, empowering users with severe motor impairments to regain a greater degree of independent movement.

ACKNOWLEDGEMENTS

The financial assistance of the National Research Foundation (NRF), the Automotive Industry Development Agency (AIDC), and the Advanced Mechatronics Technology Centre (AMTC) at Nelson Mandela University for this research is hereby acknowledged. The opinions expressed and conclusions drawn are those of the authors, and do not necessarily reflect the views of the NRF, AIDC, or AMTC.

REFERENCES

[1] **J. M. Baker**, "Gait disorders," *American Journal of Medicine,* vol. 131, no. 6, pp. 602-607, 2018. https://doi.org/10.1016/j.amjmed.2017.11.051

[2] **D. Shi, W. Zhang, W. Zhang, and X. Ding**, "A review on lower limb rehabilitation exoskeleton robots," *Chinese Journal of Mechanical Engineering,* vol. 32, no. 1, pp. 1-11, 2019. https://doi.org/10.1186/s10033-019-0389-8

[3] **N. Aliman, R. Ramli, and S. M. Haris**, "Design and development of lower limb exoskeletons: A survey," *Robotics and Autonomous Systems,* vol. 95, pp. 102-116, 2017. https://doi.org/10.1016/j.robot.2017.05.013

[4] **F. Cincotti *et al.***, "Non-invasive brain–computer interface system: Towards its application as assistive technology," *Brain Research Bulletin,* vol. 75, no. 6, pp. 796-803, 2008. https://doi.org/10.1016/j.brainresbull.2008.01.007

[5] **M. M. N. Mannan, M. A. Kamran, and M. Y. Jeong**, "Identification and removal of physiological artifacts from electroencephalogram signals: A review," *IEEE Access,* vol. 6, pp. 30630-30652, 2018. https:// /doi.org/10.1109/ACCESS.2018.2842082

[6] **X. Jiang, G. B. Bian, and Z. Tian**, "Removal of artifacts from EEG signals: A review," *Sensors,* vol. 19, no. 5, 987, 2019. https://doi.org/10.3390/s19050987

[7] **J. Xu, S. Mitra, C. van Hoof, R. F. Yazicioglu, and K. A. Makinwa**, "Active electrodes for wearable EEG acquisition: Review and electronics design methodology," *IEEE Reviews in Biomedical Engineering,* vol. 10, pp. 187-198, 2017. https://doi.org/10.1109/RBME.2017.2656388

[8] **N. Ahmad, R. A. R. Ghazilla, and M. Z. H. M. Azizi**, "Steady state visual evoked potential based BCI as control method for exoskeleton: A review," *Malaysian Journal of Public Health Medicine,* vol. 16, no. supp.1, pp. 86-94, 2016. Available: https://www.researchgate.net/publication/294836212_Steady_state_visual_evoked_potential_based_BCI_as_control_method_for_exoskeleton_A_review

[9] **M. S. Al-Quraishi, I. Elamvazuthi, S. A. Daud, S. Parasuraman, and A. Borboni**, "EEG-based control for upper and lower limb exoskeletons and prostheses: A systematic review," *Sensors,* vol. 18, no. 10, 3342, 2018. https://doi.org/10.3390/s18103342

[10] **M. Orban, M. Elsamanty, K. Guo, S. Zhang, and H. Yang**, "EEG-based movement intention recognition for lower-limb exoskeletons," *Bioengineering,* vol. 9, no. 12, 768, 2022. https://doi.org/10.3390/bioengineering9120768

[11] **S. Kalagi, J. Machado, V. Carvalho, F. Soares, and D. Matos**, "Brain computer interface systems using non-invasive electroencephalogram signal: A literature review," in *Proceedings of the 2017 International Conference on Engineering, Technology and Innovation (ICE/ITMC)*, Funchal, Portugal, 2017, pp. 1578-1583. https://doi.org/10.1109/ICE.2017.8280071

[12] **V. Bartenbach, M. Gort, and R. Riener**, "Concept and design of a modular lower limb exoskeleton," in *2016 6th IEEE International Conference on Biomedical Robotics and Biomechatronics (BioRob)*, 2016, pp. 649-654. https://doi.org/110.1109/BIOROB.2016.7523699

[13] **M. Alvarez *et al.***, "Simultaneous estimation of human and exoskeleton motion: A simplified protocol," in *2017 International Conference on Rehabilitation Robotics (ICORR)*, 2017, pp. 1431-1436. https://doi.org/10.1109/ICORR.2017.8009449

[14] **J. Oakes, R. Botta, and T. Bahill**, "Technical performance measures," in *INCOSE International Symposium*, July 2006, vol. 16, no. 1, 2006, pp. 1466-1474. https://doi.org/10.1002/j.2334-5837.2006.tb02826.x

[15] **E. López-Larraz *et al.***, "Control of an ambulatory exoskeleton with a brain–machine interface for spinal cord injury gait rehabilitation," *Frontiers in Neuroscience,* vol. 10, 359, 2016. https://doi.org/10.3389/fnins.2016.00359

[16] **O. Rosanne, I. Albuquerque, R. Cassani, J.-F. Gagnon, S. Tremblay, and T. H. Falk**, "Adaptive filtering for improved EEG-based mental workload assessment of ambulant users," *Frontiers in Neuroscience*, vol. 15, 611962, 2021. https://doi.org/10.3389/fnins.2021.611962

[17] **D. J. McFarland, W. A. Sarnacki, and J. R. Wolpaw**, "Brain–computer interface (BCI) operation: Optimizing information transfer rates," *Biological Psychology,* vol. 63, no. 3, pp. 237-251, 2003. https://doi.org/10.1016/S0301-0511(03)00073-5

[18] **I. Lipp, K. Murphy, R. G. Wise, and X. Caseras**, "Understanding the contribution of neural and physiological signal variation to the low repeatability of emotion-induced BOLD responses," *Neuroimage*, vol. 86, pp. 335-342, 2014. https://doi.org/10.1016/j.neuroimage.2013.10.015

[19] **J. F. Soriano, J. E. Rodríguez, and L. A. Valencia**, "Performance comparison and design of an optimal polycentric knee mechanism," *Journal of the Brazilian Society of Mechanical Sciences and Engineering*, vol. 42, pp. 1-13, 2020. https://doi.org/10.1007/s40430-020-02313-6

[20] **R. Barkataki, Z. Kalita, and S. Kirtania**, "Anthropomorphic design and control of a polycentric knee exoskeleton for improved lower limb assistance," *Intelligent Service Robotics,* vol. 17, pp. 555-577, 2024. https://doi.org/10.1007/s11370-024-00512-x

[21] **W. S. Lin, Y. P. Shih, and J. J. Lee**, "Design of a two-stage cycloidal gear reducer with tooth modifications," *Mechanism and Machine Theory,* vol. 79, pp. 184-197, 2014. https://doi.org/10.1016/j.mechmachtheory.2014.04.009

[22] **K. E. Mathewson, T. J. Harrison, and S. A. Kizuk**, "High and dry? Comparing active dry EEG electrodes to active and passive wet electrodes," *Psychophysiology,* vol. 54, no. 1, pp. 74-82, 2017. https://doi.org/10.1111/psyp.12536

[23] **X. Chen, Y. Wang, S. Gao, T.-P. Jung, and X. Gao**, "Filter bank canonical correlation analysis for implementing a high-speed SSVEP-based brain–computer interface," *Journal of Neural Engineering*, vol. 12, no. 4, 046008, 2015. doi: 10.1088/1741-2560/12/4/046008